Sandia National Laboratories

Assessment of Materials-Based Options for On-Board Hydrogen Storage for Rail Applications

Mark D. Allendorf, Lennie Klebanoff, Vitalie Stavila, Mathew Witman

ABSTRACT

The objective of this project was to evaluate material- and chemical-based solutions for hydrogen storage in rail applications as an alternative to high-pressure hydrogen gas and liquid hydrogen. Three use cases were assessed: yard switchers, long-haul locomotives, and tenders. Four storage options were considered: metal hydrides, nanoporous sorbents, liquid organic hydrogen carriers, and ammonia, using 700 bar compressed hydrogen as a benchmark. The results suggest that metal hydrides, currently the most mature of these options, have the highest potential. Storage in tenders is the most likely use case to be successful, with long-haul locomotives the least likely due to the required storage capacities and weight and volume constraints. Overall, the results are relevant for high-impact regions, such as the South Coast Air Quality Management District, for which an economical vehicular hydrogen storage system with minimal impact on cargo capacity could accelerate adoption of fuel cell electric locomotives. The results obtained here will contribute to the development of technical storage targets for rail applications that can guide future research. Moreover, the knowledge generated by this project will assist in development of material-based storage for stationary applications such as microgrids and backup power for data centers.

ACKNOWLEDGEMENTS

CONTENTS

This page left blank

SoCalGas Research, Development, and Demonstration Program

Applicable Subprogram and Project Area: Clean Transportation On-Board Storage.

Principal Investigator/project lead: Dr. Mark D. Allendorf, Sandia National Laboratories

Mail Stop 9161, Livermore, CA 9455-0969

Phone: (925)294-2895

Email: mdallen@sandia.gov

Project team: Dr. Lennie Klebanoff

Dr. Vitalie Stavila

Dr. Matthew Witman

ACRONYMS AND TERMS

Term	Definition
BOP	Balance of plant
BT	Benzyltoluene
CNG	Compressed natural gas
DOE	Department of Energy
EG	Ethylene glycol
FCEV	Fuel cell electric vehicle
FEA	Finite element analysis
HDV	Heavy duty vehicle
HSECoE	Hydrogen Storage Engineering Center of Excellence
ICE	Internal combustion engine
LDV	Light duty vehicle
LH_2	Liquid hydrogen
LOHC	Liquid organic hydrogen carrier
MCH	Methylcyclohexane
MDV	Medium duty vehicle
MOF	Metal-Organic Framework
MHSDT	Metal Hydride Storage Design Tool
MH	Metal hydride
OMS	Open metal site
PEMFC	Proton exchange membrane fuel cell
TEA	Techno-economic analysis

1. BACKGROUND

1.1. Prior literature on hydrogen storage for rail applications

The use of hydrogen fuel cells for rail applications has been under consideration for the past two decades. Although still at an early stage of development, the advantages of hydrogen fuel cells are clear: zero pollutant gases (only water is produced), higher efficiency than internal combustion engines (ICE) – nearly a factor of two for several rail duty cycles – and avoidance of costs associated with track electrification.[1-2] There is also evidence that maintenance costs will be lower.[2] A useful survey of the literature can be found in the thesis by R. S. Isaac.[2] In brief, several studies are relevant to the present investigation. In 2005, a mining vehicle was fielded in which hydrogen was stored in the form of a metal hydride.[3] Shortly thereafter, Miller and coworkers developed a hybrid switcher locomotive combining a fuel cell with lead-acid batteries.[4-5] Hydrogen was stored as a gas at 350 bar rather than a metal hydride, partly due to concerns regarding the combined weight of the hydride and the heavy batteries. Systems have been tested in which hydrogen was stored on board or in a tender.

However, a major barrier to the use of hydrogen as a transportation fuel is its volumetric energy density, which is significantly lower than diesel fuel (although on mass basis it is much higher than current lithium-ion batteries; Figure 1). Although high-pressure hydrogen gas is cost-competitive with batteries for HDV, the gas storage system is still a major contributor to the high cost of these vehicles, adding as much as $50,000 to the cost of a CNG-fueled truck compared with a diesel truck.[6] Consequently, there is considerable interest in developing material-based alternatives, many of which have volumetric energy densities higher than even liquid hydrogen, but lower gravimetric energy densities (Figure 1). Detailed comparisons and the use of these storage modes as a base case are discussed below.
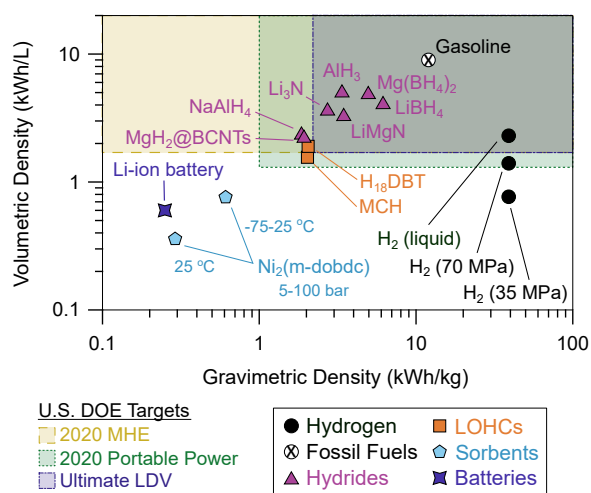
Figure 1. Comparison of the volumetric and gravimetric energy densities of hydrogen storage materials with US DOE technical targets. Adapted from Ref. 7.

2.   PROJECT DESCRIPTION AND APPROACH

2.1.   Project objective

The objective of this project was to perform a feasibility study to evaluate potential material- and chemical-based hydrogen storage modes for rail applications. To enable this analysis, we incorporated industry feedback and guidance for specific applications when available (e.g. mass and volume constraints, amount of usable hydrogen stored etc.). Non-materials-based storage (liquid and compressed gas) are considered a base case for comparison, as these are under consideration for both HDV and rail applications. The results of this analysis provide data needed for equipment design, defining technical targets, and scoping further R&D. This report constitutes the primary project deliverable. This study modeling is not a techno-economic analysis, however. Its focus is to determine whether materials-based storage of any type is capable of meeting capacity requirements within the constraints of a defined volume available for storage.

2.2.   Storage material types considered in this analysis

This section provides a summary of the properties and characteristics of the hydrogen storage materials and chemical compounds considered in the analysis. We divide these into two categories. Solid-state materials store hydrogen in the form of chemical bonds (metal hydrides) or in a physiosorbed state on a high surface-area material (e.g, nanoporous adsorbents such as MOFs). Chemical storage systems are molecular in nature and are either small organic molecules (liquid organic hydrogen carriers; LOHCs) or small molecules such as ammonia. Note that compressed natural gas (CNG) is also a chemical storage system but we do not consider it here as analyses already exist in the literature.[8]

2.2.1.   Metal hydrides

Extensive research focused on developing metal hydrides for transportation and other applications has been conducted, accelerating considerably after it was shown that the complex hydride $NaAlH_4$ could be made reversible using additives such as titanium halides.[9] Metal hydrides have several important advantages for on-board hydrogen storage:

- The volumetric capacity of many metal hydrides is higher than 700 bar compressed gas and can even exceed that of liquid hydrogen (Figure 1).[7]

- The equilibrium H_2 pressure required to regenerate a hydride storage bed is far lower than that used in high-pressure gas storage tanks (350 bar or 700 bar), reducing both safety concerns and infrastructure costs. Moreover, H_2 release from metal hydrides is thermally activated and can be tailored to match the requirements of the fuel cell. In some cases, thermal activation could be achieved, for example, using residual heat released by the proton exchange membrane (PEM) fuel cell to increase the overall energy efficiency.

- Due to their thermal stability, metal hydrides reduce the risk of leaks compared to compressed gas or liquid hydrogen (LH_2). The latter always has some associated boiloff. Leak minimization is important for safety considerations and because hydrogen is now recognized as an indirect

greenhouse gas.[10]

- Depending on the thermodynamics and kinetics of the particular hydride, full regeneration is possible following H_2 desorption, using pressures much lower than 700 bar. For example, the metal amides considered in this project can be regenerated under 100 bar hydrogen.[11] Consequently, on-board storage tanks designed to withstand ultrahigh pressures, which can. Be heavy and expensive, are not needed. Moreover, at these much lower pressures, low-cost compressors can be used, which reduces the cost of the fueling infrastructure.

- Many hydrides are comprised of light, earth-abundant elements, such as Li, B, N, Na, Mg, and Al. This makes them attractive for transportation applications due to their high gravimetric energy storage capacity, which can be an order of magnitude or more greater than batteries (Figure 1).[7] Although the additional weight of metal hydride storage relative to diesel fuel is of concern in some applications, it can be beneficial for railway traction.[12]

2.2.2. *Nanoporous adsorbents*

Nanoporous materials (pore diameters ~0.5 – 3 nm), including MOFs,[13] covalent-organic frameworks (COFs),[14] porous aromatic frameworks (PAFs),[15] and porous carbons have received extensive attention for their potential to store large quantities of gases such as hydrogen and methane. These materials can store larger amounts of hydrogen at maximum pressures ~100 bar. The weak physisorption of these molecules favors materials with high surface areas to maximize storage capacity. Among these, MOFs are perhaps the most promising because of their ultrahigh surface areas, in excess of 1000 m^2/g and tailorable pore size, geometry, and surface chemistry enabled by their crystalline structure. MOFs have the potential to meet the DOE volumetric hydrogen storage target but suffer from low gravimetric and volumetric capacities due to their generally weak isosteric heats of adsorption: < 9 kJ/mol H_2 without under-coordinated metal sites ("open metal sites"; OMS) and up to 15 kJ/mol H_2 for MOFs with OMS.[13] The record hydrogen volumetric capacity was achieved by the MOF Ni_2(m-dobdc) (m-dobdc^{4-} = 4,6- dioxido-1,3-benzenedicarboxylate), which has a capacity of 11.0 g/L at 25 °C and 23.0 g/L if a temperature swing between -75 °C and 25 °C is used.[16] This high capacity is a product of a high volumetric density of strongly binding OMS with an isosteric adsorption heat of 13.7 kJ/mol. Nevertheless, this MOF does not reach the DOE volumetric storage target and currently the only ones that do meet it require adsorption at 77 K.[17]

A recent assessment[18] of strategies for designing adsorbent materials that can meet the DOE LDV targets[19] concluded that successful materials will possess: 1) a high volumetric density of OMS and 2) binding energies in the range of 15 – 25 kJ/mol to enable storage at ambient temperatures. The latter was recently achieved in a vanadium MOF with an isosteric heat of 21 kJ/mol.[20] In addition, however, MOFs (and other high surface-area adsorbents) typically display a Type 1 adsorption isotherm[21] in which the maximum capacity is reached at pressures below the 5 bar minimum required to operate a fuel cell (Figure 2). As a result, much of the stored hydrogen is inaccessible for applications involving fuel cells. A small number of MOFs with flexible structures circumvent this problem for methane[22] and hydrogen[23] by undergoing a phase change upon gas uptake. This has the added advantage that the phase change is endothermic, which can assist with heat management. Design principles for creating flexible adsorbents for methane storage have been identified,[24] but these apply to hydrogen storage as well.
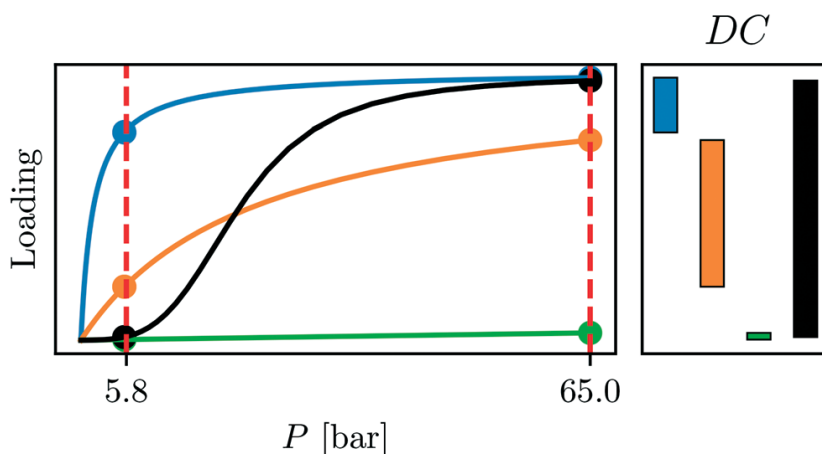
Figure 2. Example rigid material isotherms where adsorption is either too energetically favorable (blue), optimized (orange), or too unfavorable (green) for maximizing deliverable capacity. Flexible systems (black) have the potential to maximize deliverable capacity by suppressing adsorption at low pressures without sacrificing high capacity at high pressures. From Ref. 24.

2.2.3. Liquid Organic Hydrogen Carriers

LOHCs are attractive because they are readily adapted to existing infrastructure and industrial-scale processes for producing them already exist.[25-29] LOHCs in which the dehydrogenated products are liquids facilitate use of existing infrastructure, avoid formation of gas-phase species such as CO_2 and CO, and increase efficiency by avoiding transport issues associated with solids. However, reaction thermodynamics can conflict with required physical properties. For example, low melting point (< -20 °C) and vapor pressure (<0.01 atm at 50 °C) facilitate H_2 separation and low viscosity reduces pumping requirements. These properties are frequently in opposition, unfortunately. Comparing methylcyclohexane (MCH), currently under development by Chiyoda for stationary storage,[30] with other LOHCs provides a useful illustration. Although its H_2 content (47 kg H_2/m^3) is less than decalin or cyclohexane, it nevertheless is >50% higher than 350 bar compressed H_2 (~23 kg H_2/m^3). It is also a non-viscous liquid at -20 °C whereas both cyclohexane and benzene are solid at 5 °C. However, the large enthalpy for H_2 release ($\Delta H°$(dehyd) ~68 kJ/mol H_2) and its high vapor pressure at 50 °C reduce H_2 release efficiency and complicate purification.

Computational studies show that installing heteroatoms in the arene ring substantially reduces $\Delta H°$(dehyd),[31] indicating that perhydro-N-ethylcarbazole (H12-NEC; 54 kg H_2/m^3) has characteristics required for a practical hydrogen carrier. H12-NEC has a lower $\Delta H°$(dehyd) (~50 kJ/mol H_2,), a low 50 °C vapor pressure, and fast dehydrogenation kinetics with suitable catalysts. Unfortunately, its use is complicated by being a solid at room temperature, requiring strategies to maintain the liquid phase using additives or, less attractively, avoiding complete conversion.[32] Acrylics such as ethanol,[33] butanediol,[34] ethyleneglycol (EG),[35] 2-aminoethanol,[36] and aqueous formate[37-39] could circumvent these issues and balance capacity vs. favorable liquid-phase (de)hydrogenation thermodynamics. Dehydrogenation rates are much lower than for cyclic alkanes, however. The large number potential LOHC candidates is motivating the use of data science techniques to identify molecules with the desirable combination of properties.[40] Another important factor is the need for suitable catalysts for accelerating the reactions. LOHCs are by definition stable molecules that must be heated to release hydrogen, implying a non-zero activation energy. In general, the development of effective catalysts

represents the major scientific challenge to implementation of LOHCs, not the discovery of molecules with desirable intrinsic properties.

2.2.4. Ammonia

Ammonia as a hydrogen carrier possesses many of the advantages of LOHCs. Several reviews of this technology have been published,[41-43] including a techno-economic analysis (TEA) (see discussion below).[43] It is produced on an industrial scale using the Haber-Bosch process, which is highly optimized. Ammonia liquification occurs at -33 °C[41] and it can be transported using existing infrastructure and stored as a liquid at modest pressures (≥8.58 bar).[41] Its volumetric capacity is far higher than either pressurized gas or LH_2 (Table 1). Its toxicity is a disadvantage; however, anhydrous ammonia is transported in bulk by rail and safety standards are well established. Safety concerns regarding combustion are also reduced relative to other hydrogen carriers because the ammonia ignition temperature (651 °C) is higher than either liquid hydrogen (571 °C) or MCH (535 °C). From a materials perspective its biggest disadvantages are the high energy cost associated with industrial-scale production by the Haber-Bosch process, which also has large greenhouse gas emissions, and the high temperatures required to release H_2.

As a storage material ammonia can be indirect, i.e., one that must be decomposed to form hydrogen gas prior to use in a fuel cell, or direct by reforming to hydrogen in a solid oxide fuel cell (SOFC). SOFCs that reform NG to create hydrogen have been assessed as power sources for locomotives.[44] A recent TEA compared ammonia with liquid hydrogen and methylcyclohexane (MCH) as hydrogen storage materials.[43] The levelized cost of ammonia storage is projected to be lower than LH_2 or MCH. In another study, Al-Hamed et al. assessed the potential of using a hybrid solid oxide fuel cell (SOFC)/PEMFC system coupled with an ammonia dissociation and separation unit. They concluded that efficiencies over 60% can be achieved, which is more than double that of cascaded Rankine cycles.[45] Safety concerns are significant; however, an assessment of these risks concluded that they can be overcome.[46]

Table 1. Properties of representative hydrogen carriers, including gravimetric and volumetric storage density, thermodynamic values at 298.15 K for dehydrogenation, and calculated temperature to achieve 1 bar H_2 equilibrium.

Compound	Gravimetric Capacity (g H_2/kg)	Volumetric Capacity (g H_2/L)	$\Delta H°$ (kJ/mol H_2)	$\Delta S°$ (J/mol $H_2 \cdot K$)	T_{1bar} (°C)
Liquid H_2	33.3 kWh/kg[e]	70.85	0.90	130	-252.7
Gaseous H_2 (350 bar)	33.3 kWh/kg[e]	23.325[c,d]	N/A		N/A
Gaseous H_2 (700 bar)	33.3 kWh/kg[e]	39.237[c,d]	N/A		N/A
Methylcyclohexane	62	47	67	122	281
H18-DBT	62	57	65		
H12-NEC	58	54	53	117	182
Pyrrolidine	57	49	52	107	214
Piperidine	71	61	62	120	245
Ethanol	44	35	36	101	84
Butanediol	45	46	43	118	94
Ammonia	178	121	31	60	237
Formic acid	44	53	32	213	-124
Methanol[a]	189	150	44	136	47
Formate[b]	29	56	20	63	46
LiH	127	104	181	149	655
MgH_2	76	110	74	128	305
$PdH_{0.6}$	6	69	39	92	151
AlH_3	101	149	10	123	-192
$TiFeH_2$	18	111	27	107	-21
$TiCrMnH_3$	19	118	20	106	-84
$LaNi_5H_6$	15	103	32	110	18
Mg_2NiH_4	36	97	66	125	255
$TiVZrNbHfH_{12}$	24	161	62	88	431
$LiAlH_4$	78	72	8	125	-209
$NaAlH_4$	45	64	38	121	41
$LiBH_4$	119	80	72	116	348
$Mg(BH_4)_2$	124	102	56	127	168
$LiNH_2$/LiH	82	87	73	124	316
$Mg(NH_2)_2$/2LiH	42	58	44	119	96

[a]Water for steam reformation or hydrolysis is not included in computed capacities. [b]Thermodynamics are for a 1 M solution. [c]https://webbook.nist.gov/chemistry/fluid/. Accessed June 27, 2023. [d]At 25 °C. [e]1 kWh = 33.3 kg H_2.

3. RESULTS

3.1. Model system for rail applications

We considered three possible use cases in which a hydrogen-powered fuel cell would be used for rail transportation: 1) yard switcher; 2) long-haul locomotive; and 3) tender that would provide additional storage beyond what would be possible onboard the locomotive. We assume that a bounding box exists for each of these cases, as indicated in Table 2. In each case, it is assumed that the storage material is contained within 9 equal-sized cylinders, as indicated in Figure 3, where x is determined by the application or car type in which hydrogen is stored. Hydrogen storage capacity is assumed to scale linearly, allowing increased capacity by increasing the length of the cylinders or their number.
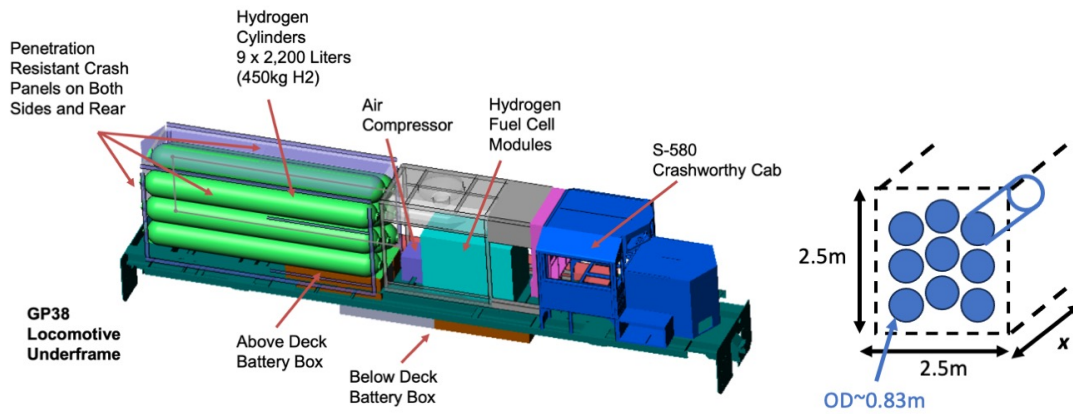
Figure 3. Generic locomotive configuration used to define the space available for hydrogen storage. The schematic above is for a yard switcher but an analogous cylinder configuration was used for the long-haul locomotive and tender. It was assumed that the entire volume of the tender was occupied by the storage tubes (i.e., no other BOP components). Used with permission from Pedro Santos, HGmotive.

Table 2. Bounding box dimensions and storage tank properties for rail use cases considered here.

Use case	Width (m)	Height (m)	Length x (m)	No. of cylinders	Cylinder OD (m)	Tank material	Max. tank pressure (bar)
Yard Switcher or local	2.5	2.5	4.0	9	0.83	A286[b]	100
Long-haul locomotive	2.5	2.5	9.7	9	0.83	A286[b]	100
Tender	2.5	2.5	24.0	9	0.83	A286[b]	100

3.2. Pressurized hydrogen gas and liquid hydrogen

For purposes of our analysis, we use hydrogen stored as a gas under high pressure (either 350 bar or 700 bar) and liquid hydrogen (LH_2) as benchmarks for comparison with material and chemical storage options. On a material basis (i.e., the gas without the associated tank and BOP) the volumetric capacity of hydrogen at 700 bar is 39.2 kg H_2 m^{-3} and 23.3 at 350-bar (Table 1). Accounting for the weight

penalty associated with the mass of the storage system reduces these by roughly a factor of two. Such penalties exist regardless of the storage material, but it is important to highlight them for pressurized gas and LH_2 due to the unique constraints imposed by these storage modes.

Although there are no DOE targets for hydrogen storage specifically related to rail applications, useful comparisons can be made with other modes of transportation. Pressurized hydrogen falls well short of the 50 g H_2/L ultimate target set by the U.S. Department of Energy (DOE) for light duty vehicles (LDV).[19] For heavy duty vehicles (HDV), designs proposed for Class 8 tractors using compressed gas technology require ~55 kg of usable hydrogen, but a steel tank to contain this pressure is estimated to weigh >9240 kg (4200 lbs) vs. 330 kg (150 lbs) for diesel fuel. The volumetric and gravimetric capacities can be increased significantly using a lighter-weight alloy such as A286.[47] The highest capacities are achieved using fiber-reinforced composite tanks (Type 3 and Type 4), but these are very costly. However, the cost of composite fiberglass tanks is decreasing and these may become competitive in the near future.[48]

The significant energy penalty required for liquefaction (~30%)[49] and the need for cryogenic storage limit the application space for LH_2. Safety concerns are also high for LH_2, particularly for long-haul operations. In such cases, it is not uncommon for locomotives to be stopped in tunnels, particularly for long unit trains in which there are locomotives in the middle of the train. A release of LH_2 under such circumstances could produce a combustible mixture within a confined space. Cryo-compressed hydrogen has a higher capacity than pressurized gas (44 g H_2 L^{-1}), but is uneconomical for some applications.[50]

3.3. Metal hydrides

The storage system simulations performed in this study employed two models. First, the Hydrogen Storage Tank Mass and Cost Estimation Model, or "Tankinator" model,[51-53] developed as part of the DOE Hydrogen Storage Engineering Center of Excellence (HSECoE), was originally developed for LDV and was used here to model tanks designed to hold high-pressure hydrogen gas.[54-55] The Metal Hydride Storage Design Tool (MHSDT)[56] was used to model metal hydride tanks is a MATLAB version of the Tankinator code that was created to consider metal hydrides and LDV, MDV, and HDV. However, it is straightforward to extend this to the storage concept in Figure 3 by specifying the dimensions of a single storage cylinder and assuming that the capacity scales with the number of cylinders (nine in this case). The HyMARC PNNL team developed this computational tool for estimating the mass and material composition for cylindrical Type 1 (various steel and aluminum alloys), Type 3 (composite with aluminum liner), and Type 4 (composite with plastic liner) hydrogen storage tanks in a Microsoft Excel format. Here, we assume that the tank is fabricated from A286 alloy, which we found in our prior analysis of a metal hydride for HDV yields the highest volumetric capacity at elevated temperatures needed to produce a minimum hydrogen pressure of 5 bar.[47]

The Tankinator and MHSDT tools provide an estimate of the mass and volume of the storage system, including the basic tank geometry and fabrication material from a limited number of geometric and temperature inputs. MHSDT also uses metal hydride properties (Table 3) to estimate the size of the entire storage system, including the metal hydride, heat exchanger, combustor, cooling tubes, and other balance of plant components. Input parameters for the system (e.g. tank dimensions, and operating pressure range) are given in Table 4. In all cases, a use of a combustor burning some of the available hydrogen is assumed to provide heat to maintain the hydride bed at a sufficient temperature to yield a minimum of 5 bar pressure. Heat transfer properties are used primarily to determine the

number of cooling tubes required during refueling, which is an exothermic process. The MHSDT estimates the necessary cylinder wall thickness for a given tank (specifying either diameter, length, or volume). The wall thickness of the cylindrical portion of the tank is primarily based on classic thin-walled pressure cylinder hoop stress formula. The end cap geometry is assumed to be perfectly hemispherical with wall thicknesses equal to the cylindrical section. Although MHSDT is only an estimation tool, its accuracy has been verified using finite element analysis (FEA) showing that the wall thicknesses predicted by the estimation tool results in an acceptable stress state. Additional details regarding the design properties associated with the four tank types and the assumptions incorporated into the metal hydride preprocessor can be found in Ref. 52.

Table 3. Properties of hydrides considered in the analysis.

Description	MgH_2 [1]	Li-Mg-N [2]	$NaAlH_4$ [3]	$LaNi_5H_6$ [4]	$TiFeH_2$ [5]
Hydrogen grav. capacity, hydride only (%)[a]	7.60	5.60	4.50	1.50	1.70
Hydrogen gravimetric capacity, composite (%)[b]	6.84	5.04	4.05	1.35	1.53
Enthalpy of desorption per mol H_2 (ΔH; J/mol)	74000	40400	40000	32000	27000
Entropy of desorption per mol (ΔS; J/mol•K)	128	114	120.9	110	110
Thermal conductivty[c] (κ; W/m•K)	3.85	3.85	3.85	3.85	3.85
Crystallographci density, metal hydride (kg/m³)	1450	1090	1256	6800	6550
Density, high TC additive[d]	2.25	2.25	2.25	2.25	2.25
Mass fraction, high TC additive[d]	0.10	0.10	0.10	0.10	0.10
Void fraction[e]	0.30	0.30	0.30	0.30	0.30
Estimated bed density[f]	914	687	791	4284	4127

1. Thermodynamic data from NIST WebBook.[57]
2. Composition: (LiNH₂ : 1MgH₂ : 0.1KH : 0.1LiH). Thermodynamic data: Sandia experimental measurements.
3. Thermodynamic data from Ref. 58.
4. Thermodynamic data from Ref. 59.
5. Thermodynamic data from Ref. 60.

[a]Theoretical max/pure hydride (I.e. bulk), or from experiment. [b] Capacity for the hydride as a composite assuming 10wt% of a thermally conducting but non hydrogen-containing material. Capacity is therefore 90% of the pure material. [c]Assumed to achievable for any hydride by appropriate mixture with a high thermal-conductivity material such as expanded natural graphite. [d]TC = thermal conductivity. [e]Typical packing fractions for metal hydride powders are ~0.7, so we assume a consistent void fraction of the hydride/high-TC composite in the hydride bed. This also allows for expansion and contraction of the bed upon hydrogenation and dehydrogenation, respectively. [f]Density of the hydride/high-TC composite in the hydride bed, assuming mixture of hydride with 10 m/m% high-TC and 0.30 void fraction of the bed.

Table 4. System design parameters used to predict the usable capacity for metal hydrides.

The calculations assume the bounding box, shown in Fig. 2 and Table 2 and are for one of the nine storage cylinders within the box. The OD of each storage cylinder is assumed to be constant at 0.83 m. The maximum length of each storage cylinder is assumed to be as shown in Table 2. The mass of usable hydrogen in each tank is then used as a fitting parameter to match the cylinder length for a switcher, long-haul locomotive, and tender.

Input design parameter	Value	Units
Mass of usable H_2 available in the tank	Fit parameter	kg
Coolant tube external radius	0.005	m
Coolant tube thickness	0.00089	m
acceptable hydride temperature rise during refueling	45	K
Upper Hydrogen Operating Pressure	100	atm
Lower Hydrogen Operating Pressure	5	atm
Hemispherical endcap option	Yes	option
Material Option	A286	option
Desired **exterior** tank length/tank diameter	Computed	
Desired tank **exterior** length Enter 0 to calculate	Computed	m
Desired tank **exterior** diameter Enter 0 to Calculate	0.83	m
Target Refueling time (300 s = DOE 2020 target)	3000	seconds
Combustion Efficiency if required	0.8	

3.3.1. General comments

As discussed above and detailed in Table 2, we assumed a fixed bounding box and tank configuration and considered three use cases: yard switcher, long-haul locomotive, and tender. The amount of usable hydrogen was computed by varying this value to achieve the maximum tank length for each use case as indicated in Table 2. The results for the yard switcher, long-haul locomotive, and tender use cases are given in Tables 5 – 7. As a general comment, the results for the long-haul locomotive likely have the highest uncertainty due to incomplete knowledge concerning the amount of space required for the fuel cell system and associated components.

Several general observations can be made that are relevant to all three use cases. First, we assumed a refueling time of 3000 s (50 min), which is a factor ten higher than the DOE LDV target but nevertheless somewhat arbitrary. Longer refueling times may be feasible. The effect of varying this is to change the system mass. Increasing the refueling time leads to modest decreases in system mass and volume due to the reduced heat management requirements (heat is released when the metal hydride is regenerated). Consequently, system capacity values increase if more time is allowed for refueling. Second, system mass, which includes the metal hydride, tank, and balance of plant (cooling tubes, burner, etc.) scales with the hydride density but is also affected by the enthalpy of hydrogen desorption (DH). Higher DH increases the heat management requirements (number of cooling tubes) and thus the system mass. System volume is unaffected as this is constrained by our bounding box assumptions. Third, in all cases, some hydrogen is burned to bring the hydride bed to the temperature required to generate a minimum of 5 bar hydrogen pressure required by the fuel cell. This affects the hydrogen utilization efficiency; MgH$_2$, with the highest enthalpy of desorption, has the lowest efficiency, whereas TiFeH$_2$ has the lowest enthalpy and highest efficiency. Finally, the maximum temperature varies strongly with the heat of desorption. In all cases except MgH$_2$, which has the highest DH, the maximum temperature is below that specified for A-286.[61]

Concerning the specific hydrides we considered, the volumetric capacity relative to 700 bar pressurized gas (labeled "% of 700 bar systems" in the tables): Assuming a Type 3 carbon fiber tank the results in Tables 5—7 show that on a system basis most of the hydrides are competitive with 700 bar pressurized gas and several considerably exceed it. In particular, $TiFeH_2$ has a volumetric capacity approaching double that of pressurized gas for all three use cases. However, this result and the prediction for the other hydrides highlights the various tradeoffs that exist to achieve a particular design goal. Among these tradeoffs are gravimetric vs. volumetric capacity; hydride and system mass; and the maximum operating temperature and associated hydrogen utilization efficiency. For example, a major design target is the amount of usable hydrogen that can be stored. Absent any other constraints, $TiFeH_2$ would be the clear winner. However, the system mass for $TiFeH_2$ is triple that of MgH_2, which has 77% of the $TiFeH_2$ usable capacity. Nevertheless, the low efficiency of hydrogen utilization for MgH_2 due to the increased heat management and balance of plant offset the capacity advantage.

3.3.2. Yard switcher

The yard switcher is predicted to be a favorable use case for hydride-based storage, as the requirement for the amount of stored hydrogen is lower than the other two (Table 5). For comparison with the literature, Hess et al. built a hydrogen fuel-cell powered switcher with 70 kg hydrogen stored in 14 roof-top tanks at 350 bar.[4, 62] The total amounts of hydrogen stored by any of the hydrides considered here in the nine-cylinder system are more than a factor of seven higher than the 70 kg of pressurized gas stored in the experimental switcher. The switcher design in Fig. 3 stores 450 kg hydrogen, but this value does not represent usable hydrogen, i.e. does not include balance of plant and tank mass. Consequently, every hydride considered is expected to store more usable hydrogen on a system basis than specified for known switcher fuel cell designs. We note that the yard switcher is also a favorable application for batteries because of the shorter duty cycles, resulting in greater dead time available for recharging. It is also somewhat more favorable for pressurized gas, as safety concerns associated with pressurized gas tanks are lower than in other use cases.

Table 5. Predicted tank dimensions, system mass, and hydride capacities for a yard switcher. Values are per cylinder (see Fig. 3) unless otherwise stated.

	MgH_2	Li-Mg-N[c]	$NaAlH_4$	$LaNi_5H_6$	$LiFeH_2$
System mass (kg)	3004	2281	2496	9432	9122
System volume (m³)	2.181	2.172	2.176	2.167	2.167
Mass H_2 Burned (kg)	50.76	14.47	13.31	19.03	17.59
Tank Outer Diameter (m)	0.86	0.86	0.86	0.86	0.86
Tank Length (m)	4.00	4.01	4.01	4.00	4.01
Number of coolant Tubes	351	135	126	167	157
Total Hydride Mass (kg)	1967	1377	1593	8534	8243
Tank Mass (kg)	910	836	838	822	805
Maximum Temperature (°C)	551	260	211	173	103
GHC (g H_2 / kg system)[a]	27.9	24.1	20.5	10.2	11.9
VHC (g H_2/ L system)[b]	38.4	25.3	23.5	44.4	50.1
% of 700 bar systems w/Type 3 tank (25.5 g/L)	150.6	99.2	92.3	174.1	196.4
% of 700 bar systems w/A286 tank (28.0 g / L)	137.2	90.3	84.0	158.5	178.9
Cylinder volume (m³)	2.329	2.319	2.331	2.314	2.313
Hydrogen utilization efficiency (%)	39.43	73.67	74.00	80.21	83.8
Mass of usable hydrogen per cylinder (kg)	83.80	54.95	51.20	96.17	108.53
Total mass usable hydrogen 9 cylinders (kg)	754	495	461	866	977
Total system mass 9 cylinders (kg)	27036	20533	22463	84889	82097

[a] Gravimetric hydrogen capacity. [b] Volumetric hydrogen capacity. [c] Composition: ($LiNH_2$: $1MgH_2$: 0.1KH : 0.1LiH).

3.3.3. Long-haul locomotive

For long-haul locomotives (Table 6), approximately 3000 kg hydrogen per locomotive are needed for continuous operation. Based on the model used here, none of the hydrides considered can meet the 3000 kg requirement for usable hydrogen per long-haul locomotive. The highest usable capacity predicted is 2477 kg from $TiFeH_2$, but this comes with a total system mass of 22982 kg. The mass of the largest freight locomotive, the SD90MAC, is 193000 kg. There is considerable uncertainty in these results due to the unknown volume requirements of the fuel cell system and the mass of structural elements required for safety. It is likely that the predicted usable hydrogen capacities are an upper limit. This points to the need for a tender for each locomotive to meet the hydrogen capacity requirements. We conclude onboard hydrogen storage for long-haul locomotives is the least likely to be feasible of the three use cases we considered.

Table 6. Predicted tank dimensions, system mass, and hydride capacities for a long-haul locomotive. Values are per cylinder (see Fig. 3) unless otherwise stated.

	MgH_2	Li-Mg-N[c]	$NaAlH_4$	$LaNi_5H_6$	$LiFeH_2$
System mass (kg)	6984	5631	6177	23806	22982
System volume (m³)	5.503	5.458	5.470	5.456	5.449
Mass H2 Burned (kg)	116.84	36.66	33.75	48.34	44.59
Tank Outer Diameter (m)	0.86	0.86	0.86	0.86	0.86
Tank Length (m)	9.70	9.69	9.71	9.69	9.71
Number of coolant Tubes	327	135	126	167	157
Total Hydride Mass (kg)	4528	3490	4038	21674	20901
Tank Mass (kg)	2207	2020	2025	1990	1946
Maximum Temperature (°C)	551	260	211	173	103
GHC (g H_2 / kg system)[a]	27.6	24.7	21	10.3	12
VHC (g H_2/ L system)[b]	35.1	25.5	23.7	44.8	50.5
% of 700 bar systems w/Type 3 tank (25.5 g/L)	137.5	100.0	93	175.6	198.1
% of 700 bar systems w/A286 tank (28.0 g / L)	125.2	91.1	84.7	159.9	180.4
Cylinder volume (m³)	5.651	5.605	5.617	5.603	5.595
Hydrogen utilization efficiency (%)	39.43	73.67	74	80.21	83.8
Mass of usable hydrogen per cylinder (kg)	192.9	139.23	129.79	244.26	275.19
Total mass usable hydrogen 9 cylinders (kg)	1736.1	1253.07	1168.11	2198.34	2476.71
Total system mass 9 cylinders (kg)	62858	50675	55596	214253	206841

[a] Gravimetric hydrogen capacity. [b] Volumetric hydrogen capacity. [c] Composition: ($LiNH_2$: $1MgH_2$: 0.1KH : 0.1LiH).

3.3.4. *Tender*

The maximum carrying capacity of heavy axle freight cars is 129700 kg (286000 lbs), which is valid on the majority of U.S. track, with a gross rail car weight of 143200 kg (315000 lbs). On this basis, only the Li-Mg-N amide could be used at its maximum capacity. Alternatively, if the goal is to achieve a carrying capacity equivalent to 700 bar pressurized gas, then scaling these numbers shows that both MgH_2 and Li-Mg-N amide can store an equivalent amount of hydrogen as 700 bar pressurized gas while staying at or below the weight limit. Given uncertainties associated with tank design and storage system BOP requirements, $NaAlH_4$ may also be a feasible storage material. However, a significant unknown is the mass of the empty tender. We assumed 13200 kg,[63] but this may be an underestimate given structural reinforcements needed to meet safety requirements.

Table 7. Predicted tank dimensions, system mass, and hydride capacities for a tender. Values are per cylinder (see Fig. 3) unless otherwise stated.

	MgH$_2$	Li-Mg-N[c]	NaAlH$_4$	LaNi$_5$H$_6$	LiFeH$_2$
System mass (kg)	17753	14305	15694	61000	58757
System volume (m^3)	14.069	13.969	13.987	13.968	13.919
Mass H$_2$ Burned (kg)	299.88	94.13	86.57	124.19	114.30
Tank Outer Diameter (m)	0.86	0.86	0.86	0.86	0.86
Tank Length (m)	24.40	24.39	24.42	24.40	24.40
Number of coolant Tubes	327	135	126	167	157
Total Hydride Mass (kg)	11622	8961	10358	55678	53572
Tank Mass (kg)	5551	5087	5093	5011	4891
Maximum Temperature (°C)	551	260	211	173	103
GHC (g H$_2$/kg system)[a]	27.9	25	21.2	10.3	12
VHC (g H$_2$/L system)[b]	35.2	25.6	23.8	44.9	50.7
% of 700 bar systems w/Type 3 tank (25.5 g/L)	138	100.4	93.3	176.2	198.7
% of 700 bar systems w/A286 tank (28.0 g/L)	125.7	91.4	85.0	160.4	181.0
Cylinder volume (m^3)	14.217	14.116	14.134	14.115	14.065
Hydrogen utilization efficiency (%)	39.43	73.67	74	80.21	83.8
Mass of usable hydrogen per cylinder (kg)	495.08	357.52	332.94	627.46	705.35
Total mass usable hydrogen 9 cylinders (kg)	4456	3218	2996	5647	6348
Total system mass 9 cylinders (kg)	159777	128746	141242	548996	528813
% max cargo capacity (130000 kg)	123%	99%	109%	422%	407%
Tot. system mass for 9 A286 cylinders/scaled to be equivalent to 700 bar (kg)	115780	128233	151385	311575	266136
Tender gross mass[d]	128980	141433	164585	324775	279336
Amount over (under) max tender mass (kg)	-14200	-1747	21405	181595	136156
% over (under) max tender mass	90%	99%	115%	227%	195%

[a] Gravimetric hydrogen capacity. [b] Volumetric hydrogen capacity. [c] Composition: (LiNH$_2$: 1MgH$_2$: 0.1KH : 0.1LiH). [d] Assume mass of empty tender is 13200 kg and max gross mass is 143200 kg for heavy duty axle rail car. See https://www.up.com/aboutup/reference/maps/allowable_gross_weight/index.htm for info on gross rail car weights and cargo capacity.

3.4.   Nanoporous adsorbents

In the context of hydrogen storage for rail applications, we are not aware of any published work concerning MOFs or adsorbents more generally. However, a recent TEA study provides a basis for evaluating the potential of these materials for rail. This work focused on the transport of bulk hydrogen from one point to another rather than on-board storage for an FCEV.[64] However, the conclusions are relevant to onboard storage for rail transportation, particularly if a tender is considered to increase storage capacity. The authors of this study concluded that the levelized cost of long-distance transmission using MOFs is substantially higher than transport by compressed gas (at either 350 bar or 700 bar) or LH$_2$. Notable contributors to this cost differential are the cost of the gas terminal and the truck, both of which must operate cryogenically (at 77 K) to maximize capacity. The cost of the MOF itself is a minor component of the levelized cost. Moreover, the volumetric capacity of MOFs, even if a pressure-temperature swing is invoked, is inferior to many other materials-based storage systems, as is evident in Figure 1. Reducing this cost will likely require developing new MOFs that have higher volumetric capacity and can store the gas at temperatures approaching ambient. Achieving these would reduce the cost of both the refueling/storage terminal and the on-board storage system by reducing or eliminating the need for cryogenic storage. However, research to develop MOFs with these properties is on the cutting edge of the scientific field and represent major

synthetic challenges. For these reasons we conclude that MOFs and other adsorbents (which we expect to have similar levelized cost) are not economical compared with pressurized gas storage.

3.5. Liquid organic hydrogen carriers

We modeled the catalytic production of hydrogen by dehydrogenating an LOHC using a reactor code developed by HyMARC.[65] The system required to perform this chemistry is much more complex than that needed to dehydrogenate a metal hydride bed. In the latter, only thermal energy is required to raise the equilibrium vapor pressure of hydrogen above the material to $\geq$ 5 bar. In contrast, LOHCs require a flow reactor in which the catalytic dehydrogenation reaction occurs and the dehydrogenated products are collected in a separate reservoir. Consequently, the number of input parameters is much larger than required for modeling a metal hydride; these are listed in Appendix 1. Important specifications include the locomotive average and maximum power requirements, the efficiency of the fuel cell stack, the thermodynamics and kinetics of the reaction, and the catalyst loading. Calculations were run for a fixed reactor volume corresponding to the maximum length for a given use case shown in Table 3. The code then calculates the total usable hydrogen.

Currently, rate expressions describing the dehydrogenation kinetics of many LOHCs are not well established. However, we recently published data for the dehydrogenation of ethylene glycol (EG),[66] which is an attractive carrier due to its low cost and well-established, large-volume production. The dehydrogenation reaction and the associated catalyst are shown in Figure 4.

Model predictions for the yard switcher use case are shown in Figure 5. The maximum reactor temperature and usable hydrogen capacity per liter of the system are shown as a function of EG conversion. In addition, the boiling points of EG and several other LOHCs are shown as horizontal lines. It is evident that to maintain a reactor temperature below the boiling point of EG the conversion must be limited to ~20%. The corresponding system usable capacity of ~0.008 kg/L is far below that of 700 bar pressurized gas (~20 kg/L system assuming a 50% penalty to scale from the volumetric capacity on a material basis given in Table 1).
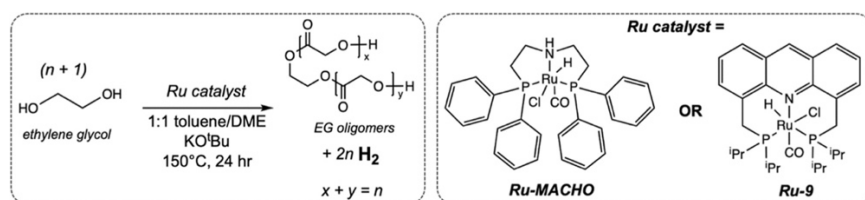
Figure 4. Catalytic reaction for dehydrogenation of EG using ruthenium organometallic complexes.[66]

Although we lack kinetic data for the dehydrogenation of the other LOHCs shown in Figure 5, an important qualitative conclusion can be made. Assuming identical dehydrogenation kinetics for all LOHCs shown, we can eliminate MeOH, EtOH, and MCH, as well as EG from consideration, as the conversions are all impractically low at temperatures below their boiling point. Only benzyltoluene (BT) has a conversion above 70% below its boiling point, but to achieve this a reactor temperature approaching 280 °C is required, which will reduce hydrogen utilization efficiency (i.e., how much hydrogen must be burned to maintain the reactor temperature). The assumption of equal kinetics is obviously incorrect. However, we can assume that the H_2 production rate for a particular use case is achievable given a sufficiently active catalyst, or equivalently, that the reactor temperature can be increased arbitrarily to achieve that rate. Reasoning then from a purely thermodynamic perspective, all of these LOHCs have large positive dehydrogenation enthalpies (Table 1). Hydrogen desorption enthalpies in Table 1 are >50 kJ/mol H_2 with the exception of the small alcohols. Coupling the $\Delta H°$ with the expected non-zero activation energy for hydrogen release indicates that dehydrogenation kinetics will be rate-limiting for the flow reactor design conditions assumed here. Although alcohols such as ethanol have the lowest $\Delta H°$, they also have the highest vapor pressures and lowest boiling points. In summary, all other things being equal, the boiling point alone could be sufficient to disqualify a given LOHC from use. Notably, this conclusion is valid for all applications, including stationary use cases, not just rail.
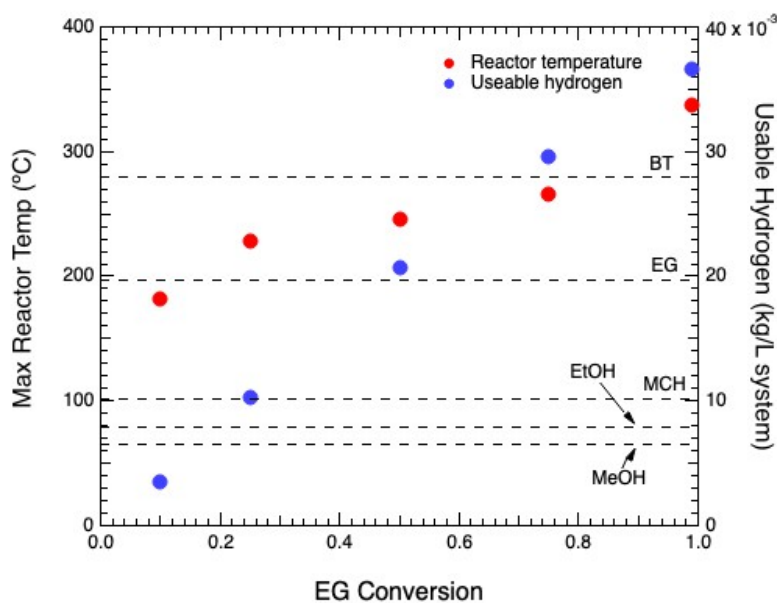
Figure 5. Predicted maximum reaction temperatures and volumetric usable hydrogen on a system basis predicted for EG dehydrogenation.

4.   CONCLUSIONS

This analysis has focused on assessing the potential of various material- or chemical-based media as an alternative to pressurized hydrogen gas or LH_2. The approach is based on predicting storage capacities based on material properties and not costs, as would be evaluated by TEA. Though of limited scope, the results provide useful insight into the feasibility for rail applications. Using pressurized hydrogen at 700 bar as the benchmark, we assessed the potential of metal hydrides, nanoporous sorbents, LOHCs, and ammonia for storage in three use cases: yard switchers, long-haul locomotives, and tenders.

Metal hydrides appears to have the greatest likelihood to be a successful alternative to pressurized gas for rail applications. This class of storage materials is the most technically mature of those considered here. Assuming a fixed volume available for the storage tank allows a comparison with pressurized gas, showing that several hydrides have volumetric capacity exceeding 700 bar. However, it appears likely that volumetric considerations will be secondary to gravimetric constraints. High-capacity hydrides such as $TiFeH_2$ are also heavy, leading to gross weight for a tender exceeding the maximum allowable on U.S. track. Consequently, the most attractive hydrides are those with the highest gravimetric capacities: MgH_2 and lithium-magnesium amide.

Of the remaining storage options considered (LOHCs, nanoporous sorbents, and ammonia), LOHCs and sorbents are less mature. Concerning LOHCs, the chief limitation of LOHCs, in contrast with metal hydrides, is not gravimetric or volumetric capacity, but the temperature required to drive the dehydrogenation reaction. These liquid reactants must remain below their boiling point, which our simulations suggest is not possible while simultaneously achieving high conversions. This conclusion must be considered preliminary, however. The dehydrogenation kinetics of some of the most prominent LOHC candidates are not well established and are also dependent on the catalyst used. Platinum-based catalysts are being used in current state-of-the-art LOHC systems such as that under development by Chiyoda. However, these are costly, operate at high temperatures, and may require hydrogen-cofeed to minimize coking, which reduces the amount of hydrogen available for storage. For sorbents, although these have not been assessed for HDV or rail, a TEA that considered MOFs for bulk hydrogen transport concluded that this would not be economical. The limitations in this case are the projected cost of the MOF and the need for cooling within a pressure/temperature-swing cycle. Finally, the capacity of liquid ammonia exceeds that of any of the storage options considered here and is transported safely in large quantities by rail. However, the dearth of dehydrogenation catalysts that can operate at moderate temperatures is the major stumbling block to widespread utilization as a hydrogen carrier. Using ammonia directly to fuel a SOFC may be the best way around this problem in the short term.

In summary, materials-based hydrogen storage for rail deserves further consideration as an alternative to pressurized gas, LH_2, or cryo-compression. An essential next step is to conduct TEA of specific materials or liquid carriers for specific use cases. This will require direct involvement of the rail industry to define system design requirements, which is already occurring, and several assessments and demonstration projects are underway. The results of the present study provide valuable input for these activities and to the DOE, which through HyMARC and within its Energy Materials Network[67] is performing the research and development necessary to enable clean, affordable hydrogen as a versatile energy carrier.

REFERENCES

1. Hoffrichter, A.; Hillmansen, S.; Roberts, C., Conceptual propulsion system design for a hydrogen-powered regional train. *IET Electrical Systems in Transportation* **2016,** *6* (2), 56-66.
2. Isaac, R. S. Fuels and Fuel Technologies for Powering 21st Century Passenger and Freight Rail: Simulation-Based Case Studies in a U.S. Context. UC Davis: Institute of Transportation Studies, Davis, CA, 2020.
3. Delabbio, F. C.; Eastick, D.; Graves, C.; Sprott, D.; MacKinnon, T.; Betournay, M. C., Fuel cell risk assessment, regulatory compliance, and implementation of the world's first fuel cell-powered mining equipment at the Campbell Mine. *Cim Bulletin* **2005,** *98* (1087), 76-76.
4. Miller, A. R.; Hess, K. S.; Barnes, D. L.; Erickson, T. L., System design of a large fuel cell hybrid locomotive. *Journal of Power Sources* **2007,** *173* (2), 935-942.
5. Miller, A. R.; Peters, J.; Smith, B. E.; Velev, O. A., Analysis of fuel cell hybrid locomotives. *Journal of Power Sources* **2006,** *157* (2), 855-861.
6. Laughlin, M.; Burnham, A. *Case Study: Natural-Gas-Fueled Regional Transport Trucks*; U.S. Department of Energy: August 2016, 2016.
7. Allendorf, M. D.; Stavila, V.; Snider, J. L.; Witman, M.; Bowden, M. E.; Brooks, K.; Tran, B. L.; Autrey, T., Challenges to developing materials for the transport and storage of hydrogen. *Nat. Chem.* **2022,** *14* (11), 1214-1223.
8. Martinez, A. S.; Brouwer, J.; Samuelsen, G. S., Comparative analysis of SOFC-GT freight locomotive fueled by natural gas and diesel with onboard reformation. *Applied Energy* **2015,** *148*, 421-438.
9. Bogdanović, B.; Schwickardi, M., Ti-doped alkali metal aluminium hydrides as potential novel reversible hydrogen storage materials1Invited paper presented at the International Symposium on Metal–Hydrogen Systems, Les Diablerets, August 25–30, 1996, Switzerland.1. *Journal of Alloys and Compounds* **1997,** *253-254*, 1-9.
10. Cooper, J.; Dubey, L.; Bakkaloglu, S.; Hawkes, A., Hydrogen emissions from the hydrogen value chain-emissions profile an impact to global warming. *Science of the Total Environment* **2022,** *830*.
11. Garroni, S.; Santoru, A.; Cao, H. J.; Dornheim, M.; Klassen, T.; Milanese, C.; Gennari, F.; Pistidda, C., Recent Progress and New Perspectives on Metal Amide and Imide Systems for Solid-State Hydrogen Storage. *Energies* **2018,** *11* (5).
12. Hoffrichter, A. Hydrogen as an energy carrier for railway traction. University of Birmingham, Birmingham, 2013.
13. Suh, M. P.; Park, H. J.; Prasad, T. K.; Lim, D.-W., Hydrogen Storage in Metal–Organic Frameworks. *Chemical Reviews* **2012,** *112* (2), 782-835.
14. Furukawa, H.; Yaghi, O. M., Storage of Hydrogen, Methane, and Carbon Dioxide in Highly Porous Covalent Organic Frameworks for Clean Energy Applications. *Journal of the American Chemical Society* **2009,** *131* (25), 8875-8883.
15. Dawson, R.; Cooper, A. I.; Adams, D. J., Nanoporous organic polymer networks. *Progress in Polymer Science* **2012,** *37* (4), 530-563.
16. Kapelewski, M. T.; Geier, S. J.; Hudson, M. R.; Stuck, D.; Mason, J. A.; Nelson, J. N.; Xiao, D. J.; Hulvey, Z.; Gilmour, E.; FitzGerald, S. A.; Head-Gordon, M.; Brown, C. M.; Long, J. R., M-2(m-dobdc) (M = Mg, Mn, Fe, Co, Ni) Metal-Organic Frameworks Exhibiting Increased Charge Density and Enhanced H-2 Binding at the Open Metal Sites. *Journal of the American Chemical Society* **2014,** *136* (34), 12119-12129.
17. García-Holley, P.; Schweitzer, B.; Islamoglu, T.; Liu, Y.; Lin, L.; Rodriguez, S.; Weston, M. H.; Hupp, J. T.; Gómez-Gualdrón, D. A.; Yildirim, T.; Farha, O. K., Benchmark Study of Hydrogen Storage in Metal–Organic Frameworks under Temperature and Pressure Swing Conditions. *ACS Energy Letters* **2018,** *3* (3), 748-754.
18. Allendorf, M. D.; Hulvey, Z.; Gennett, T.; Ahmed, A.; Autrey, T.; Camp, J.; Cho, E. S.; Furukawa, H.; Haranczyk, M.; Head-Gordon, M.; Jeong, S.; Karkamkar, A.; Liu, D. J.; Long, J. R.; Meihaus, K. R.; Nayyar, I. H.; Nazarov, R.; Siegel, D. J.; Stavila, V.; Urban, J. J.; Veccham, S. P.; Wood, B. C.,

An assessment of strategies for the development of solid-state adsorbents for vehicular hydrogen storage. *Energy & Environmental Science* **2018,** *11* (10), 2784-2812.

19. Target Explanation Document: Onboard Hydrogen Storage for Light-Duty Fuel Cell Vehicles. https://www.energy.gov/eere/fuelcells/downloads/target-explanation-document-onboard-hydrogen-storage-light-duty-fuel-cell.

20. Jaramillo, D. E.; Jiang, H. Z. H.; Evans, H. A.; Chakraborty, R.; Furukawa, H.; Brown, C. M.; Head-Gordon, M.; Long, J. R., Ambient-Temperature Hydrogen Storage via Vanadium(II)-Dihydrogen Complexation in a Metal-Organic Framework. *Journal of the American Chemical Society* **2021,** *143* (16), 6248-6256.

21. Thommes, M.; Kaneko, K.; Neimark, A. V.; Olivier, J. P.; Rodriguez-Reinoso, F.; Rouquerol, J.; Sing, K. S. W., Physisorption of gases, with special reference to the evaluation of surface area and pore size distribution (IUPAC Technical Report). *Pure and Applied Chemistry* **2015,** *87* (9-10), 1051-1069.

22. Mason, J. A.; Oktawiec, J.; Taylor, M. K.; Hudson, M. R.; Rodriguez, J.; Bachman, J. E.; Gonzalez, M. I.; Cervellino, A.; Guagliardi, A.; Brown, C. M.; Llewellyn, P. L.; Masciocchi, N.; Long, J. R., Methane storage in flexible metal-organic frameworks with intrinsic thermal management. *Nature* **2015,** *527* (7578), 357-+.

23. Choi, H. J.; Dinca, M.; Long, J. R., Broadly hysteretic H-2 adsorption in the microporous metal-organic framework Co(1,4-benzenedipyrazolate). *Journal of the American Chemical Society* **2008,** *130* (25), 7848-+.

24. Witman, M.; Ling, S. L.; Stavila, V.; Wijeratne, P.; Furukawa, H.; Allendorf, M. D., Design principles for the ultimate gas deliverable capacity material: nonporous to porous deformations without volume change. *Molecular Systems Design & Engineering* **2020,** *5* (9), 1491-1503.

25. Aaldto-Saksa, P. T.; Cook, C.; Kiviaho, J.; Repo, T., Liquid organic hydrogen carriers for transportation and storing of renewable energy - Review and discussion. *J. Power Sources* **2018,** *396*, 803-823.

26. Gianotti, E.; Taillades-Jacquin, M.; Roziere, J.; Jones, D. J., High-Purity Hydrogen Generation via Dehydrogenation of Organic Carriers: A Review on the Catalytic Process. *ACS Catalysis* **2018,** *8* (5), 4660-4680.

27. Modisha, P. M.; Ouma, C. N. M.; Garidzirai, R.; Wasserscheid, P.; Bessarabov, D., The Prospect of Hydrogen Storage Using Liquid Organic Hydrogen Carriers. *Energy Fuels* **2019,** *33* (4), 2778-2796.

28. Niermann, M.; Beckendorff, A.; Kaltschmitt, M.; Bonhoff, K., Liquid Organic Hydrogen Carrier (LOHC) - Assessment based on chemical and economic properties. *Int. J. Hydrog. Energy* **2019,** *44* (13), 6631-6654.

29. Preuster, P.; Papp, C.; Wasserscheid, P., Liquid Organic Hydrogen Carriers (LOHCs): Toward a Hydrogen -free Hydrogen Economy. *Acc. Chem. Res.* **2017,** *50* (1), 74-85.

30. Kurosaki, D. Introduction of Liquid Organic Hydrogen Carrier and the Global Hydrogen Supply Chain Project. https://www.energy.gov/sites/prod/files/2018/10/f56/fcto-infrastructure-workshop-2018-32-kurosaki.pdf.

31. Clot, E.; Eisenstein, O.; Crabtree, R. H., Computational structure-activity relationships in H-2 storage: how placement of N atoms affects release temperatures in organic liquid storage materials. *ChemCommun.* **2007,** (22), 2231-2233.

32. Cheng, H.; Wu, J.; Dong, Y.; Yang, M. Liquid hydrogen storage system 20180065849A1, 2015.

33. Tran, B. L.; Johnson, S. I.; Brooks, K. P.; Autrey, S. T., Ethanol as a Liquid Organic Hydrogen Carrier for Seasonal Microgrid Application: Catalysis, Theory, and Engineering Feasibility. *ACS Sustainable Chemistry & Engineering* **2021,** *9* (20), 7130-7138.

34. Onoda, M.; Nagano, Y.; Fujita, K., Iridium-catalyzed dehydrogenative lactonization of 1,4-butanediol and reversal hydrogenation: New hydrogen storage system using cheap organic resources. *Int. J. Hydrog. Energy* **2019,** *44* (53), 28514-28520.

35. Zou, Y. Q.; von Wolff, N.; Anaby, A.; Xie, Y. J.; Milstein, D., Ethylene glycol as an efficient and reversible liquid-organic hydrogen carrier. *Nat. Catal.* **2019,** *2* (5), 415-422.

36. Hu, P.; Fogler, E.; Diskin-Posner, Y.; Iron, M. A.; Milstein, D., A novel liquid organic hydrogen

carrier system based on catalytic peptide formation and hydrogenation. *Nature Communications* **2015,** *6* (1), 6859.

37. Grubel, K.; Jeong, H.; Yoon, C. W.; Autrey, T., Challenges and opportunities for using formate to store, transport, and use hydrogen. *J. Energy Chem.* **2020,** *41*, 216-224.

38. Grubel, K.; Su, J.; Kothandaraman, J.; Brooks, K.; Somorjai, G. A.; Autrey, T., Research Requirements to Move the Bar forward Using Aqueous Formate Salts as H2 Carriers for Energy Storage Applications *J. Energy Power Technol.* **2020,** *2* (4).

39. Su, J.; Lu, M.; Lin, H. F., High yield production of formate by hydrogenating CO_2 derived ammonium carbamate/carbonate at room temperature. *Green Chem.* **2015,** *17* (5), 2769-2773.

40. Paragian, K.; Li, B.; Massino, M.; Rangarajan, S., A computational workflow to discover novel liquid organic hydrogen carriers and their dehydrogenation routes. *Molecular Systems Design & Engineering* **2020,** *5* (10), 1658-1670.

41. Hasan, M. H.; Mahlia, T. M. I.; Mofijur, M.; Fattah, I. M. R.; Handayani, F.; Ong, H. C.; Silitonga, A. S., A Comprehensive Review on the Recent Development of Ammonia as a Renewable Energy Carrier. *Energies* **2021,** *14* (13).

42. Lamb, K. E.; Dolan, M. D.; Kennedy, D. F., Ammonia for hydrogen storage; A review of catalytic ammonia decomposition and hydrogen separation and purification. *International Journal of Hydrogen Energy* **2019,** *44* (7), 3580-3593.

43. Wijayanta, A. T.; Oda, T.; Purnomo, C. W.; Kashiwagi, T.; Aziz, M., Liquid hydrogen, methylcyclohexane, and ammonia as potential hydrogen storage: Comparison review. *International Journal of Hydrogen Energy* **2019,** *44* (29), 15026-15044.

44. Brouwer, J.; Azizi, A. *Thermodynamic and Dynamic Assessment of Solid Oxide Fuel Cell Hybrid Systems for Use in Locomotives*; DOT/FRA/ORD-19/16; 2019.

45. Al-Hamed, K. H. M.; Dincer, I., A novel ammonia solid oxide fuel cell-based powering system with on-board hydrogen production for clean locomotives. *Energy* **2021,** *220*, 119771.

46. Duijm, N. J.; Markert, F.; Paulsen, J. L. *Safety assessment of ammonia as a transport fuel*; Risoe-R No. 1504(EN); Risø National Laboratory: Risø, Denmark, 2005.

47. Allendorf, M. D.; Horton, R.; Stavila, V.; Witman, M. *Assessment of tank designs for hydrogen storage on heavy duty vehicles using metal hydrides*; SAND2023-05851; Sandia National Laboratories: 2023.

48. Shin, H. K.; Ha, S. K., A Review on the Cost Analysis of Hydrogen Gas Storage Tanks for Fuel Cell Vehicles. *Energies* **2023,** *16* (13).

49. Petitpas, G.; Aceves, S., Hydrogen Storage in Pressure Vessels: Liquid, Cryogenic, and Compressed Gas. In *Hydrogen Storage Technology, Materials and Applications*, Klebanoff, L. E., Ed. Taylor and Francis: Boca Raton, 2012; p 97.

50. Ahluwalia, R. K.; Huaa, T. Q.; Peng, J. K.; Lasher, S.; McKenney, K.; Sinha, J.; Gardiner, M., Technical assessment of cryo-compressed hydrogen storage tank systems for automotive applications. *International Journal of Hydrogen Energy* **2010,** *35* (9), 4171-4184.

51. Hydrogen Materials Advanced Research Consortium: Hydrogen Storage Systems Modeling. https://www.hymarc.org/models.html.

52. Klymyshyn, N. A.; Barrett, N. P. *PNNL Tank Mass Estimator for Cross Comparison of Type 1, Type 3, and Type 4 Pressure Vessels ("Tankinator")*; PNNL-SA-179141; Pacific Northwest National Laboratory: Richland, WA, 2022.

53. Sprik, S.; Brooks, K.; Grady, C.; Thornton, M. Hydrogen Storage System Modeling: Public Access, Maintenance, and Enhancements. https://www.hydrogen.energy.gov/pdfs/review22/st008_thornton_2022_p.pdf.

54. Hydrogen Storage Engineering Center of Excellence. https://www.energy.gov/eere/fuelcells/hydrogen-storage-engineering-center-excellence (accessed Feb. 7, 2023).

55. Motyka, T. *Hydrogen Storage Engineering Center of Excellence Metal Hydride Final Report*; 2014.

56. Brooks, K. P.; Sprik, S. J.; Tamburello, D. A.; Thornton, M. J., Design tool for estimating metal

hydride storage system characteristics for light-duty hydrogen fuel cell vehicles. *International Journal of Hydrogen Energy* **2020,** *45* (46), 24917-24927.

57. NIST Chemistry WebBook. https://webbook.nist.gov/chemistry/). (accessed accessed 12 August, 2022).

58. Schüth, F.; Bogdanović, B.; Felderhoff, M., Light metal hydrides and complex hydrides for hydrogen storage. *Chemical Communications* **2004,** (20), 2249-2258.

59. Hubbard, W. N.; Rawlins, P. L.; Connick, P. A.; Stedwell, R. E.; O'Hare, P. A. G., The standard enthalpy of formation of LaNi5 The enthalpies of hydriding of LaNi5−xAlx. *The Journal of Chemical Thermodynamics* **1983,** *15* (8), 785-798.

60. Dematteis, E. M.; Berti, N.; Cuevas, F.; Latroche, M.; Baricco, M., Substitutional effects in TiFe for hydrogen storage: a comprehensive review. *Materials Advances* **2021,** *2* (8), 2524-2560.

61. San Marchi, C.; Somerday, B. P. *Technical Reference for Hydrogen Compatibility of Materials*; SAND2012-7321; Sandia National Laboratories: 2012.

62. Hess, K. S.; Miller, A. R.; Erickson, T. L.; Dippo, J. L. In *Demonstration of a Hydrogen Fuel-Cell Locomotive*, 2010.

63. Allowable Gross Weight Shipments. https://www.up.com/aboutup/reference/maps/allowable_gross_weight/index.htm (accessed Oct. 28, 2023).

64. Anastasopoulou, A.; Furukawa, H.; Barnett, B. R.; Jiang, H. Z. H.; Long, J. R.; Breunig, H. M., Technoeconomic analysis of metal-organic frameworks for bulk hydrogen transportation. *Energy & Environmental Science* **2021,** *14* (3), 1083-1094.

65. Brinkerhoff, K., Model for simulating a catalytic flow reactor for LOHC dehydrogenation. Personal communication,. 2023.

66. Hellman, A. N.; Torquato, N. A.; Foster, M. E.; Dun, C.; Reynolds, J. E., III; Yu, C. J.; Tran, A. D.; Shivanna, M.; Garcia, G. F. H.; Yang, J.; Chen, Y.; Su, J.; Urban, J. J.; Allendorf, M. D.; Stavila, V., Heterogenization of Homogeneous Ruthenium(II) Catalysts for Carbon-Neutral Dehydrogenation of Polyalcohols. *ACS Applied Energy Materials* **2023,** *6* (14), 7353-7362.

67. Energy Materials Network. https://www.energy.gov/eere/energy-materials-network/about-energy-materials-network (accessed Oct. 29, 2023).

APPENDIX A.   INPUT PARAMETERS FOR SIMULATING LOHC AND LOHC DEHYDROGENTATION REACTOR

Input parameter		Units
Molecular weight LOHC	62.08	g/mol
Wt Fraction H_2 in the LOHC	0.0487	--
Number of Reactions to Model (1 or 2)	1	--
Reaction Enthalpy Rxn 1 (negative=exothermic)	23200	J/mol H_2
Molar Ratio H_2 maximum for CH material Rxn 1	1.5	mol H_2/mol CH
Pre-exponential factor for Rxn 1	3.13E+13	sec-1
Activation Energy for Rxn 1	123985.2	J/mol H_2
Exponent for Avrami or Reaction Order for Rxn 1	2	--
Reaction Enthalpy Rxn 2 (negative=exothermic)	0	J/mol H_2
Molar Ratio H2 maximum for CH material Rxn 2	0	mol H_2/mol CH
Pre-exponential factor for Rxn 2	0	sec-1
Activation Energy for Rxn 2	0	J/mol H_2
Exponent for Avrami or Reaction Order for Rxn 2	1	--
Weight fraction inert with LOHC Material to Slurry	0	--
Heat Capacity LOHC Material	2742	J/kg/K
Heat Capacity inert slurrying agent	0	J/kg/K
Heat Capacity LOHC Material Product	1950	J/kg/K
Density LOHC Material	1113.2	kg/m3
Density inert slurrying agent (can't be zero)	-1	kg/m3
Density LOHC Material Product	1533	kg/m3
Molar Concentration of impurity 1	0	ppm
Adsorbent maximum loading impurity 1	0	g impurity/g adsorbent
Molecular weight impurity 1	0	g/mol
Molar Concentration of impurity 2	0	ppm
Adsorbent maximum loading impurity 2	0	g impurity/g adsorbent
Molecular weight impurity 2	0	g/mol
Mass of usable hydrogen required	20	kg
Total system volume required	25	m3
Maximum Hydrogen Storage H_2 Production Required	3000	kW
Average Hydrogen Storage H_2 Production Required	1000	kW
Ballast Tank Pressure Initial Condition and Setpoint	30	bar
Reactor heater per length	3.00E+05	
Maximum acceptable reactor temperature	400	°C
Number of reactor tubes	3	
Number of slurry radiator tubes	15	
Number of H_2 gas radiator tubes	10	
Number of recuperator tubes (if applicable, required for endothermic reaction)	1	
conversion target	0.99	
Maximum acceptable length	9.7	m
total catalyst mass	0.012146	kg

DISTRIBUTION

Email—Internal

Name	Org.	Sandia Email Address
Kristin Hertz	8367	klhertz@sandia.gov
Christian Mailhiot	8340	cmailhi@sandia.gov
Richard Karnesky	8341	rakarne@sandia.gov
Vitalie Stavila	8341	vnstavi@sandia.gov
Matthew D. Witman	8341	mwitman@sandia.gov
Robert Horton	8367	rdhort@sandia.gov
Lennie E. Klebanoff	8367	lekeba@sandia.gov
Technical Library	1911	sanddocs@sandia.gov

Email—External

Name	Company Email Address	Company Name
Jeffrey P. Chase	JChase@socalgas.com	SoCalGas

This page left blank